Combining borehole characterization and various seismic measurements in tunnelling
Combinando la caracterización de pozos de sondeo y distintas mediciones sísmicas en la construcción de túneles

Nick Barton
Nick Barton & Associates, Oslo, Norway

Abstract

Cross-disciplinary examples of rock mass classification and characterization are selected from a recent major review by the author, from various civil engineering construction projects, with emphasis on tunnelling, and making much use of cross-hole seismic measurements and refraction seismic. The links between velocity and rock quality, deformability, permeability and velocity are developed and demonstrated. The combined use of seismic and Q-logging, allows classification and characterization to be distinguished, the former with an excavation EDZ, the latter pre-construction.

Resumen

Ejemplos multi-disciplinarios de clasificación y caracterización de masa rocosa son seleccionados de un importante estudio reciente realizado por el autor, y de varios proyectos de construcción de ingeniería civil, haciendo énfasis en la construcción de túneles, y con un amplio uso de mediciones sísmicas transversales a los pozos y estudios de refracción sísmica. Este documento desarrolla y demuestra las relaciones existentes entre velocidad y calidad de roca, grado de deformación, permeabilidad y velocidad. El uso combinado de perfilaje sísmico y de Q permite que la clasificación y caracterización tengan un sello distintivo, el primero con excavación EDZ, y el segundo previo a la construcción.

INTRODUCTION

Rock mass classification has come to be associated with the need to select a rock mass class on the basis of prior classification or rating of various rock mass parameters. Most frequently, classification is used in association with tunnel support, and also as a basis for payment. It may also reflect a need for pre-treatment. Implicit here is the existence of the tunnel, and the effect this may have on the expected rock mass response, in particular that within the EDZ. All of the above may also apply to rock slopes, but here post-treatment is more likely.

Rock mass characterization reflects a broader mission to describe the character of a rock mass where a future project is likely to be realized. Besides rock quality description with one of the standard measures such as RQD, or RMR, or Q, or GSI, or several of these, it should also include site characterization fundamentals such as rock stress, water pressure, permeability and seismic velocities. Ideally each of the above should be measured as a function of depth and azimuth and of course reflect lateral variation and variation in specific domains. Various simple index parameters of the matrix and joint sets can also considered characterization, like UCS and the JRC-JCS roughness-strength character that can be estimated during core logging.

Cross-disciplinary characterization involving Q, velocity, permeability, and deformability will be used to illustrate the frequent differences between classification and characterization.

THE EXCAVATION DISTURBED ZONE

The cross-hole seismic description of the site for a future ship lock shown in Figure 1 (diagram a) can be considered one form of characterization of the site. The RQD, RMR and Q-values of the first two cores would be essential supplementary data. Ideally core or subsequent borehole logging should be oriented due to kinematic stability assessment needs. Subsequent cross-hole seismic between supplementary holes shows the

increasing development of an EDZ actually much better than our rock mass classification would be capable of, and the 1 year delay between c) and d) would be hard to emulate with (predicted) reductions of RQD, RMR and Q.

Nevertheless, in principal we should be able to characterize this site, and classify support needs using the above parameters. An iterative element arises if through our choice of a conservative rock class, we support in two stages: at half-depth and at full-depth. The former would influence the latter, and both would perhaps prevent the degradation seen with 1 year of delay in the right-hand diagram.

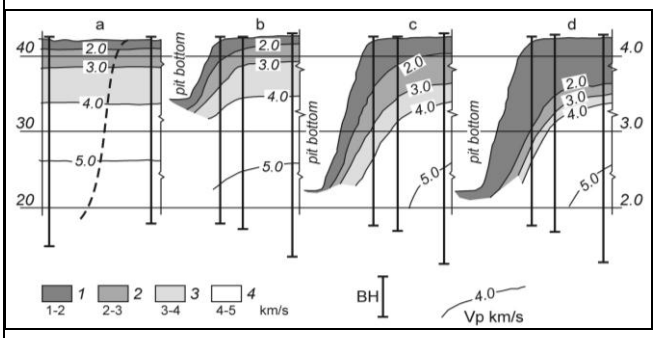

Fig. 1. Cross-hole site characterization (left), and monitoring of ship-lock excavation stages. There is a 1 year delay between diagrams c) and d). Savich et al. 1983.

An EDZ of partially different character is illustrated in Figure 2, again involving cross-hole seismic, but with both improved and reduced velocity as a result of excavation. The tangential stress concentration raises the maximum velocity by almost 1 km/s about 1 m into the wall of this 5 m diameter tunnel, and the 'negative' aspect of the EDZ reduces the velocity by a similar amount. Mean velocities were 3.5, 5.5 and 4.5 km/s, the latter in the undisturbed rock mass.

In the present context we should refer to 4.5 km/s as the simple seismic characterization of the site, perhaps corresponding to a Q-value of 10, or less than 10 if the depth is greater than 25 m or so (see later). The 3.5 km/s 'EDZ-result' should be predictable by a correct application of the SRF operator in the Q-system, and perhaps by D in GSI. However, the latter has no stress term or link to velocity, as in the case of Qc. One would perhaps need to be conditioned or trained to assume a reduced RQD as an additional measure of conservative classification, for subsequent selection of support needs, since the damaged rock will need supporting.

We see immediately that there is a potential hazard in using the seismic velocity as a measure of rock quality, if we do not take the stress level into account. Joints that are more tightly closed by the tangential stress are likely to result in higher deformation modulus due to higher normal stiffness, each of these contributing to the 1 km/s increase in seismic (P-wave) velocity. Yet we must acknowledge that rock quality per se has not improved, unless we link this with stress level.

a)

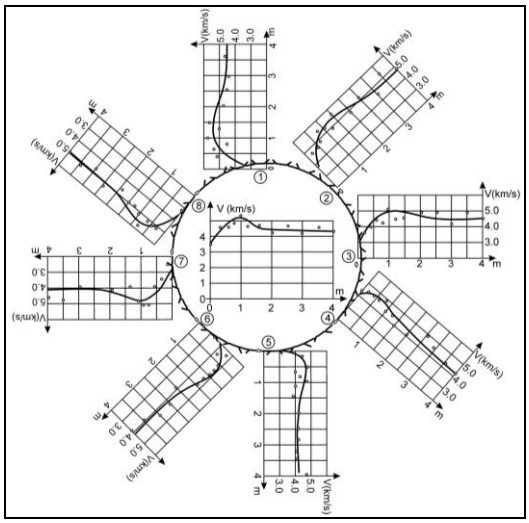

b)

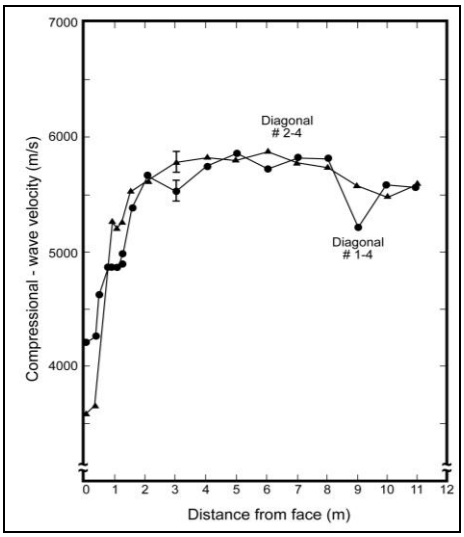

Fig. 2. a) Cross-hole seismic performed at a pressure tunnel by Kujundzíc et al., 1970.

Mean velocities of 3.5, 5.5 and 4.5 km/s are seen in the visible EDZ, in the invisible tangentially stressed EDZ, and in the undisturbed zone. The combined effect of the reduced radial stress, and the increased tangential stress are matched rather well by the spatial variations of V_P. b) Example of the increased EDZ often seen in drill-and-blast tunnels: cross-hole measurements in basalts. King et al. 1984.

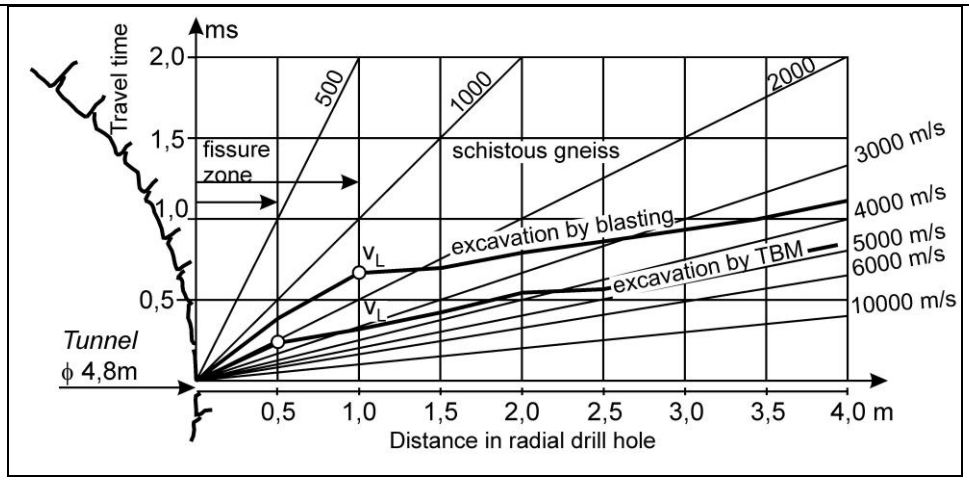

Fig. 3. Contrasting EDZ effects on Vp from drill-and-blast and TBM excavated shaft. Note combination plot with travel-time and velocity. Bonapace, 1983.

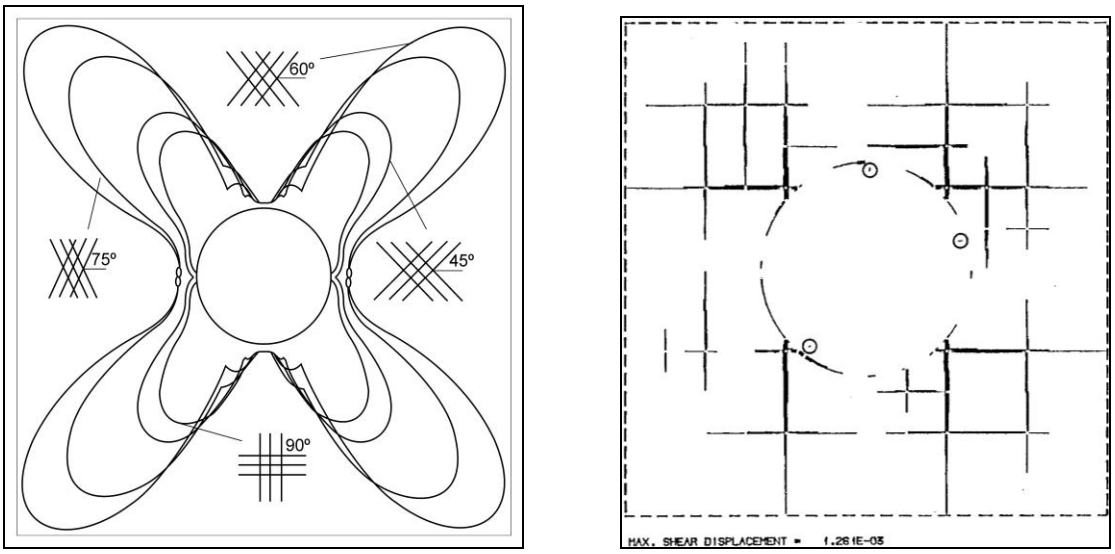

Fig. 4. Sectors where shearing may affect the details of EDZ classification. Mohr-Coulomb solutions from Shen and Barton, 1997, and an early UDEC-BB model from Christianson, 1985.

A further example of EDZ measurements in a combined plot of drill-and-blast and TBM excavations is given in Figure 3. The more pronounced (more velocity-reduced) EDZ in the case of drill-and-blast is nicely documented.

In theory, we might also expect reduced permeability at 1 m depth in the four sectors of an excavation where shear stresses do not arise, and potentially increased permeability in the sectors that may suffer some shearing, mostly close to the excavation. The existence of shear stress in four sectors is illustrated in Figure 4, first in the classic Mohr-Coulomb solutions given by Shen and Barton, 1997, and by simple UDEC-BB models of circular tunnels, from Christianson (pers. comm.. 1985). The case shown is with equal horizontal and vertical stress.

Seismic characterization of an interbedded marl-sandstone sequence at a dam site in Italy was described by Oberti et al., 1979, using both cross-hole and sonic logging in three vertical boreholes. A rather good comparison was noted, with velocities oscillating, according to rock layer, between 4.0 and 5.5 km/s within the 30 m measured depth. However, a need to relate velocity to deformability was also required, and in Figure 5 we may note an interesting problem of EDZ classification in an adit at the same site, with modulus depending on direction of loading and on depth of measurement, and all the measurements apparently affected by an EDZ.

A supplementary question we may ask is whether our frequently used RQD, RMR and Q parameters would be able to capture the differences seen in Figure 5.

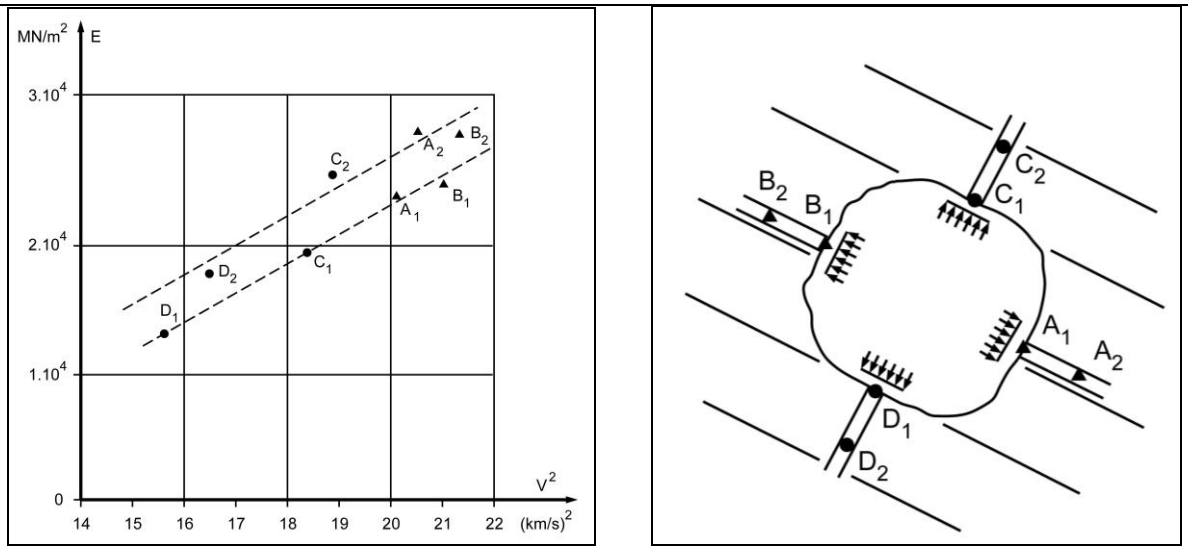

Fig. 5. Classification of the EDZ of an exploratory gallery using plate-loading, sonic logging, and MPBX recordings to relate results to specific depths. The anisotropic (orthotropic) marl-sandstone sequence exposed in the gallery provided deformation moduli varying from about 13 to 27 GPa, and sonic velocities varying from about 4 km/s to 4.6 km/s, meaning at the lower end of the pre-gallery characterization results. Oberti et al.,1979.

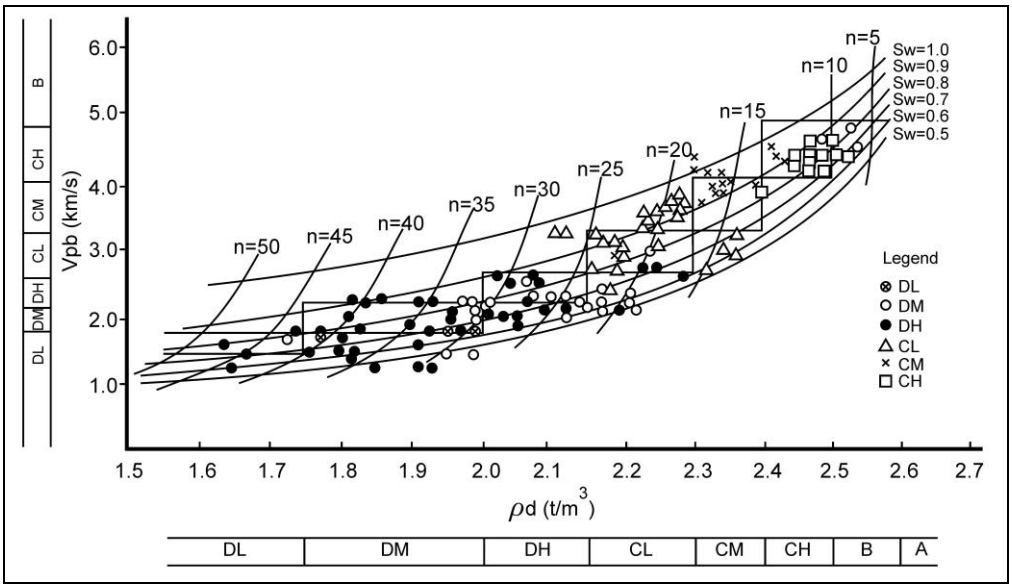

Fig. 6. Rock mass velocities linked to rock class in the Japanese Highways scheme, with extension into the low class (D_L, D_M, and D_H). Honshu-Shikoku Bridges investigations, mostly in weathered Tertiary granites. Ishikawa et al. 1995.

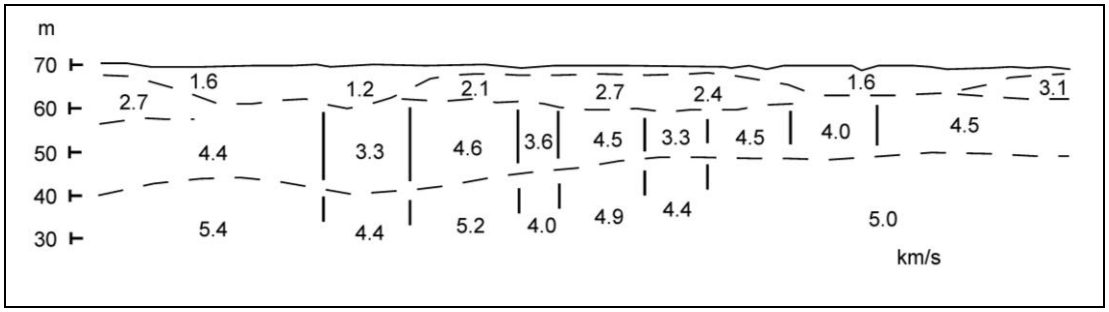

Fig. 7. An example of shallow seismic refraction results for Vp from Sjøgren et al., 1979.

EXTRAPOLATING QUALITY USING SEISMIC INVESTIGATIONS

The richness of seismic and index test data for understanding the characteristics of a site are very well illustrated in the Japanese studies for the Honshu-Shikoku Bridges, that are reproduced in part, in Figure 6. The Japanese Highways rock mass classification at the lower end of the quality scale, mostly in Tertiary granites, is particularly well demonstrated, with a selection of index data including water content (SW), porosity (n), and density.

Foundation sizes as large as 50 and even 100 m in plan, yet requiring resistance to contact pressures as high as 1 and 2 MPa were needed beneath the sea. Seismic-velocity based methods were used for extrapolating in situ deformation tests performed more readily on land, to offshore sites using down-hole pressure-meter and velocity logging.

Shallow refraction seismic and preliminary link to Q

The classic results of shallow refraction seismic shown in Figure 7 suggest a shallow soil cover and a medium depth of weathering and/or more jointed rock in the upper 20 m. Zones of higher joint frequency (rather than weaker rock) continuing to greater depth, probably cause the lower velocities to also occur at greater depth. But confirmation with boreholes, and use of the seismic for intrapolating between the boreholes is a more ideal investigation strategy, leading as it does to the possibility of cross-hole investigations, including tomographic detail (where structures have suspiciously low velocity), and of course immediate access for the performance of down-hole measurements, especially permeability measurement.

We will now concentrate attention on the possibilities of using one of the frequently used rock mass quality descriptors (the Q-system) to link with seismic velocity, starting with shallow refraction seismic such as illustrated in Figure 7. Utilization of RQD from complementary boreholes drilled beneath the seismic profiles will also be included. An excellent starting point is the extensive investigations presented by Sjøgren et al. (1979), who used shallow refraction seismic profiles (totalling 113 km) and local core logging results (totalling 2.9 km of core) to derive the following mean trends for hard rocks.

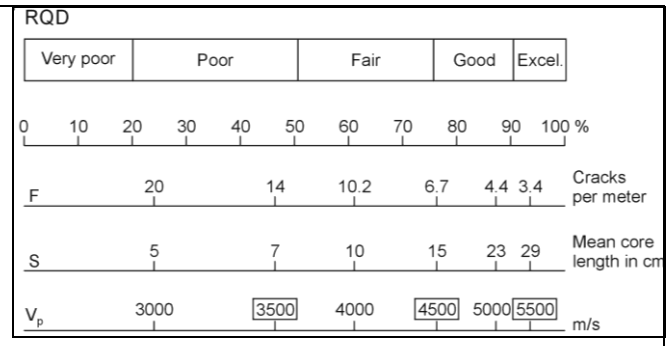

Fig. 8. Shallow refraction seismic at predominantly hard rock sites in Scandinavia. Sjøgren et al. (1979) combined 113 km of seismic profiles and 2.9 km of core logging to derive these mean trends.

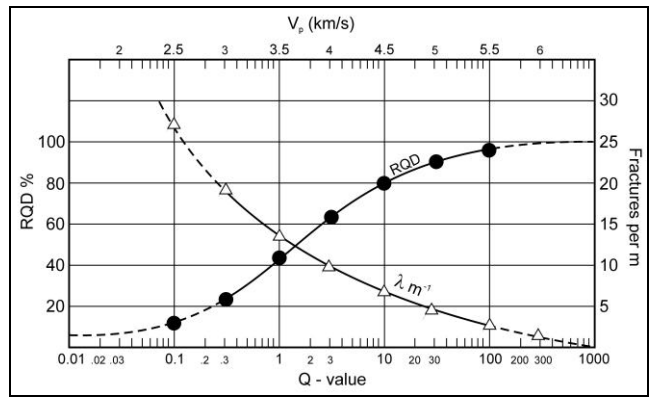

Fig. 9. Mean RQD and joint ('crack') frequency trends as a function of shallow seismic refraction measurements. Data derived from Sjøgren et al., 1979, with the addition of a Q-scale from Barton, 1995.

Using a slightly liberal smooth extrapolation (dotted lines in Figure 9), we can present this data in graphical form, and also add the Barton, 1995 addition of a Q-value scale. The latter was derived by trial and error, following several years of collecting refraction seismic velocity data at sites where core (and exposures) had been Q-logged, often by the author, or by colleagues.

For the velocity-Q links that follow, a useful first step is to 'linearize' the velocity-quality relation, with appended RQD and joint frequency (λ m-1 or F m-1) data, as in Figure 10. The simple initial relation $VP \approx 3.5 + \log Q$ may be noted. Note that the data and linkages shown in Figures 8, 9 and 10 all apply to shallow refraction seismic in essentially hard rock sites with low matrix porosities.

Two useful and very simple sets of data for introducing the next more general linkages between seismic velocity and Q are shown in Figures 11a and b. The fundamental influence of

the classic link between velocity and density, is in these cases reflected by the component of density: porosity, and a less 'pure' resultant property: uniaxial compressive strength, both intimately interconnected of course.

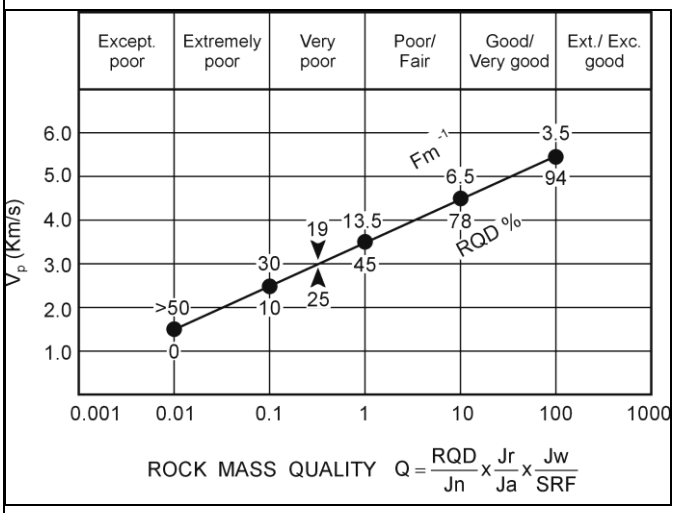

Fig. 10. Hard rock, shallow seismic refraction, mean trends from Sjøgren et al. (1979). The Q-scale was added by Barton (1995), using the hard rock correlation $V_p \approx 3.5 + \log Q$.

The more generalized relation between Q and velocity is shown in Figure 12. This development was described in Barton, 2002, and it has been demonstrated in numerous contexts in Barton, 2006. It will be noted that Q has been normalized in order to better correlate with a wider variety of weaker (and stronger) rocks. In essence Q is adjusted to smaller or larger values, termed Q_C depending on whether the rock matrix has lower or higher uniaxial compression strengths than 100 MPa. Porosity is also accounted for in approximate terms.

Figure 12 shows that depth adjustment (+ve) and porosity adjustment (-ve) are provided, based on a wider collection of seismic cross-hole tomography data from several countries, also from weaker porous rocks such as chalks and chalk marls. Deformation modulus based on plate loading and back-calculation of shaft and tunnel deformation monitoring is also appended on the right hand side, with an adjusted scale (E_{min}), for poorly explained lower values of modulus E_{mass} not sufficiently captured in site description, but presumably connected with the EDZ problem, as demonstrated in Figure 5.

An approximate support pressure scale is also shown (based on a mean Jr = 2 applied in the independently-derived Barton et al. 1974 support pressure formulation). A comparison with the deformation modulus scale in the adjacent column of Figure 12 suggests inverse proportionality between support pressure and deformation modulus. This is logical, but the simplicity is nevertheless surprising.

a)

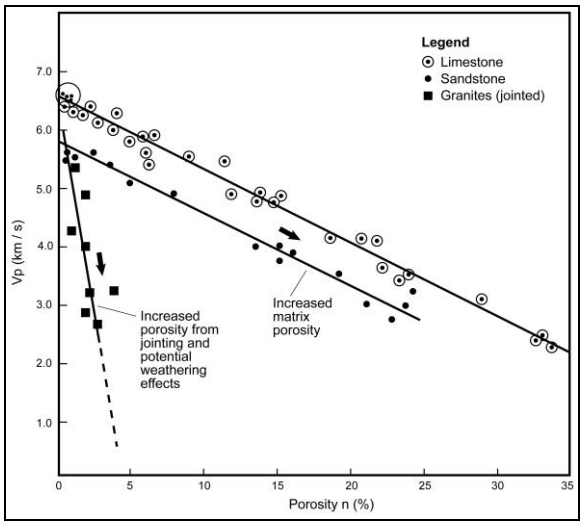

b)

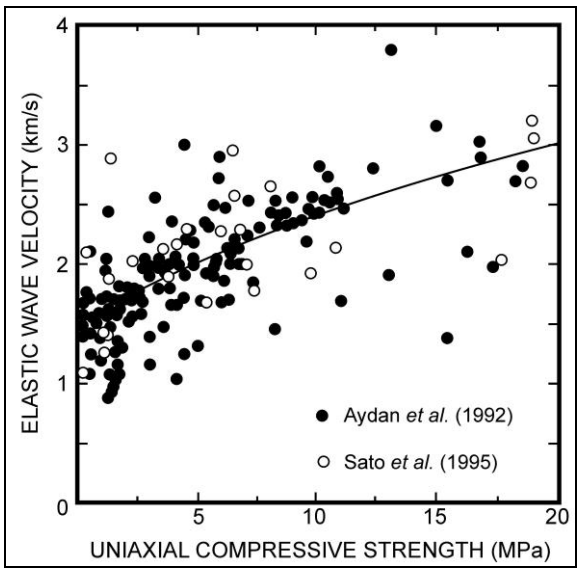

Fig. 11 a) Selection of a single rock type, and exploration of the effect of porosity show clear linear trends with velocity, in this data from Fourmaintraux, 1975. b) Uniaxial compressive strength alone, for mudstones and sandstones, from Aydan et al., 1992 and Sato et al., 1995, show much larger scatter, because of the porosity (and density) differences involved in these weak, weathered rocks.

Figure 12 demonstrates that it is important in rock mechanics modelling to allow for the increased moduli of deformation with depth or stress level. There will be other changes with depth, especially in the context of high-level nuclear waste isolation

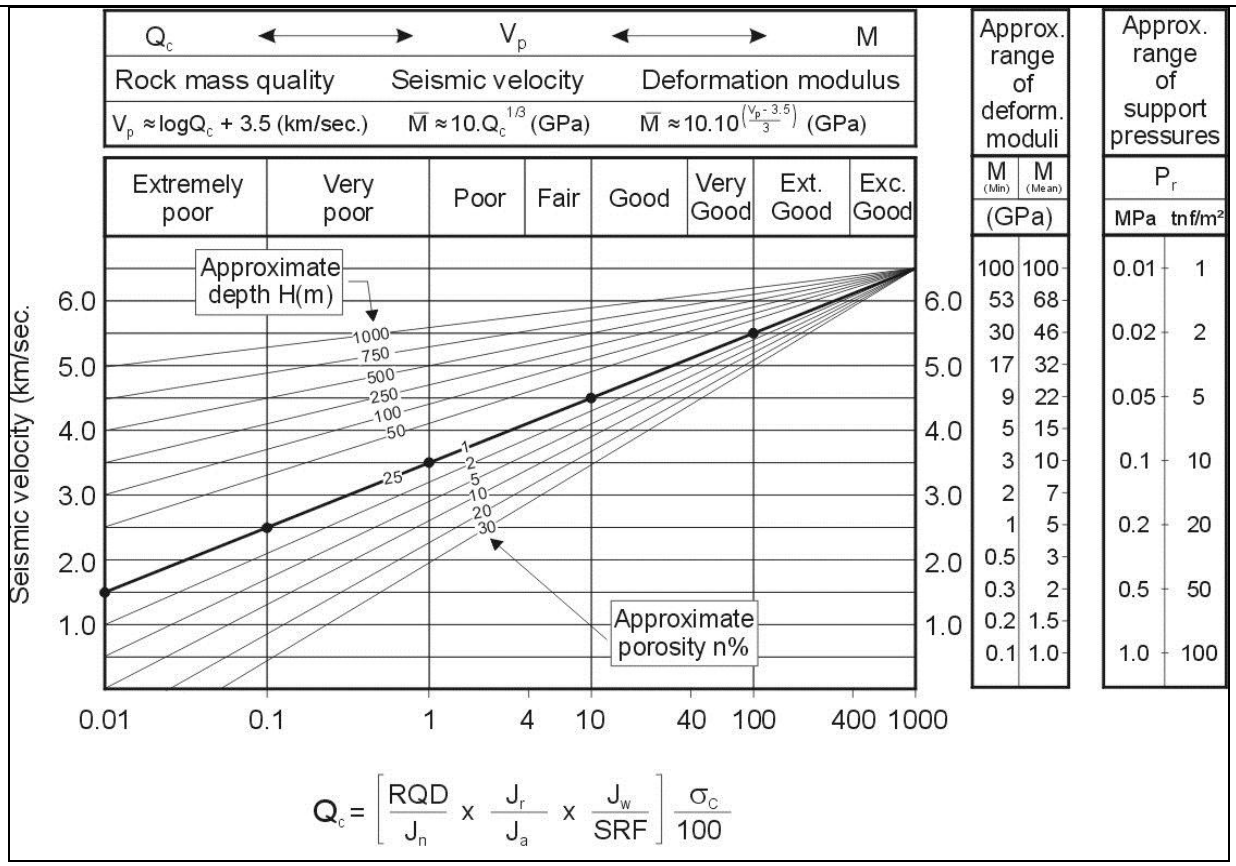

Fig. 12. An integrated empirical model for linking Q-value (via Qc) to P-wave velocity, depth, matrix porosity, and deformation modulus. Barton 2002, 2006.

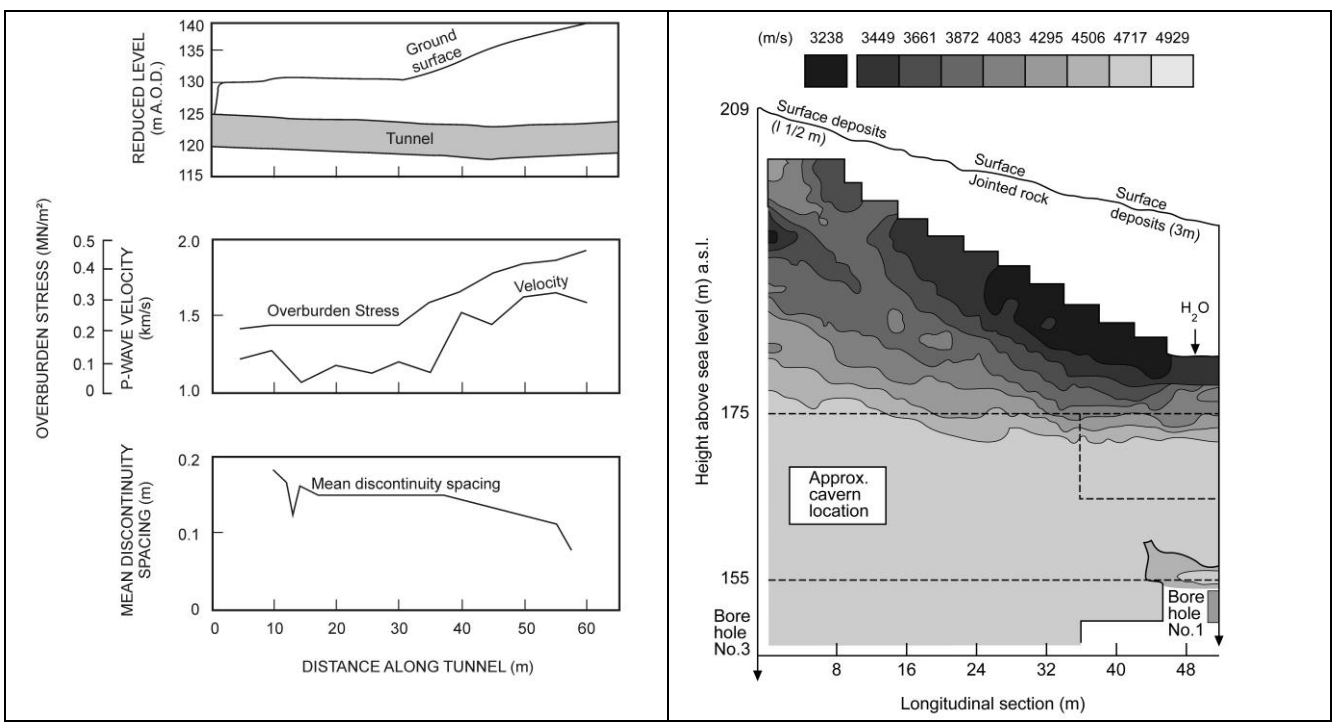

Fig. 13. a) Conclusive proof of the effect of stress increase on seismic velocity (and also modulus) with increased depth, despite greater joint frequency at depth. Hudson et al., 1980. b) Cross-hole seismic tomography at the Gjøvik cavern site, showing a strong velocity increase with depth. Analysis of adjacent boreholes gave no indication of improved RQD, or less jointing with depth. Barton et al. 1994.

due to thermal over-closure of joints. So far, such aspects do not generally seem to be accounted for in numerical modelling. Barton, 2007.

A large number of velocity depth profiles are given in Barton, 2006, based on a wide review of geophysics literature. It is common to read that the upper 50 m of the weathered crust are considered the most difficult to characterize in seismic investigations, and in fact the strong velocity gradients considerably affect the modelling of velocity at greater depths. By chance this is also the 50 m that commonly apply in our rock engineering dam foundations, shallow tunnels and portals, and in deep foundations for bridges and large buildings.

Occasionally, a set of velocity data may demonstrate the depth or stress effect, without the nagging doubt about the actual effect of the improved qualities that may accompany the depth increase. Important data from the Chinnor Tunnel in Lower Chalk (Hudson et al., 1980) are reproduced in Figure 13a. The moderately increased overburden produced an expected velocity increase, yet in this case the joint frequency actually *increased* with depth. Stress increase alone apparently caused the increase in V_p.

An example of the seismic tomography observed at the Gjøvik cavern site is reproduced in Figure 13b. Despite no systematic increase in RQD or decrease in joint frequency λ (m^{-1}), or increase in Q-value in the first 60 meters, the P-wave velocity increased by almost 2 km/s adjacent to this vertical borehole. The key to understanding this strong depth effect is that both the minor, and especially the major horizontal stress increased by several MPa over the same depth interval. The predominant (J_r = 3) joint sets in the 60 to 90 MPa tectonized gneiss were of the steeply dipping, conjugate variety. These were rapidly becoming acoustically 'closed' by the high horizontal stresses.

In Figure 14 a velocity-depth diagram has been derived from the empirical model data of Figure 12, that provides individual velocity-depth gradients for specific Q_c rock classes, where Q = Q_c in the case of UCS ≈ 100 MPa. This diagram helps to explain why faulted rock ahead of a deep tunnel may sometimes be 'invisible' or of such 'high' velocity, like 4 km/s that it is misinterpreted (Barton, 2006). It may subsequently cause tunnel collapse, or trap a TBM. In fact such rock is still probably displaying an important contrast to the surrounding rock mass. In the case of soft rock, acoustic closure probably will prevent such differentiation.

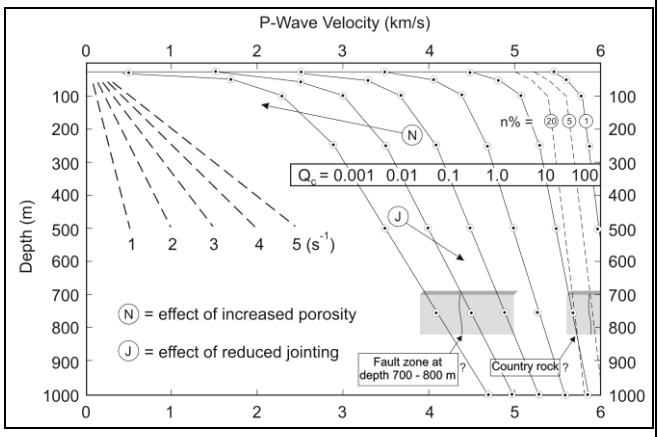

Fig. 14. The depth-velocity trends for different Qc values. Barton (2006). VP – depth gradients (s-1) tend to be in double-figures or even triple figures (e.g. 200 s-1) in the top 25 m due to 'Q-jumping'. This should be borne in mind when interpreting the results of VP, so as not to over-estimate the rock quality or Q-value, such as in the case of faults ahead of tunnels. (Barton, 2007).

In general, 'Q-jumping' will be experienced when progressing downwards to greater depth, i.e. rock qualities tend to improve, giving steeper V_P – depth (s^{-1}) gradients. This will partly be a function of reduced weathering and clay content in discontinuities, and partly due to changed rock types. In fact this will also apply to another 'Q' factor, the seismic Q or inverse of attenuation that geophysicists have used for at least 40 years to describe *their* concept of 'rock quality', specifically *seismic quality*. So seismic Q, or Q_{seis} to distinguish it from Q_{rock}, will also be found to 'Q-jump' in the upper tens of meters. Numerous examples of Q_{seis} from many different depths, and from different disciplines and effective stress levels, are given by Barton, 2006.

An example of Q-jumping in basically one (basaltic) rock type to a depth of 1000 m is given in Figure 15. This is from a mid-ocean East Pacific Rise 'wide aperture profile' from Kappus et al. 1995. It is chosen because of the rarity of measurements to such depth in one rock type. However there is a complication of pillow lavas, dykes and sills within these young basalts. The 'Q-jumping' was interpreted by Barton, 2006, by plotting the rapidly increasing velocities with depth, specifically in the first 500 m depth. Reducing porosity, increased age, and increasing hydrothermal sealing of joints and fractures seems to be the cause of the interpreted quality improvements.

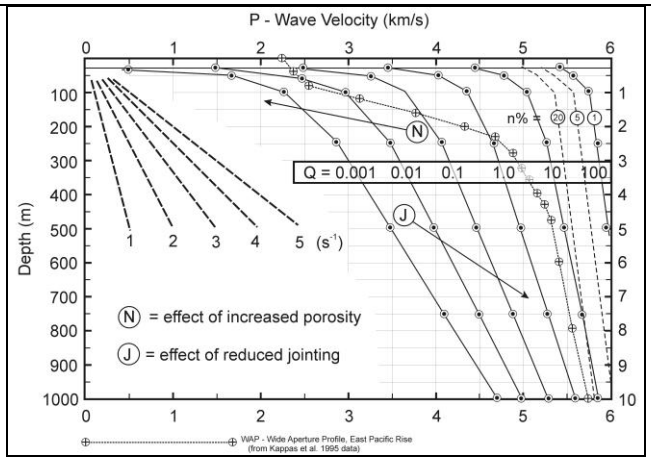

Fig. 15. Rapidly increasing P-wave velocities in sub-ocean basalts to at least 500 m depth, due to reducing matrix and joint-related porosity, increasing age, and increased hydrothermal sealing of tectonic joint structures. Velocity data from Kappus et al., 1995.

RELATING PERMEABILITY TO Q AND TO Q_{H20}

Pre-measurement estimation of permeability from rock mass characterization at any given depth is never easy, and may indeed be inadvisable, since there are potential problems such as flow-channels within the joint planes that have suffered erosion or solution-effects, and there are joints that may be clay-sealed, therefore having both low permeability and low Q-value.

For hard, low porosity, jointed rock masses without clay, the approximate Lugeon scales shown in Figure 16 may have some practical merit, when 'out in the field' in a tunnelling situation, and needing, for example, to assess pre-grouting needs. Table 1 shows a collection of potential inter-relationships derived from this figure, where 'proving them wrong' is also useful, as anomalies may thereby be uncovered and test needs identified. Where clay is present, a greater level of sophistication is needed than that shown in Table 1, or in this figure.

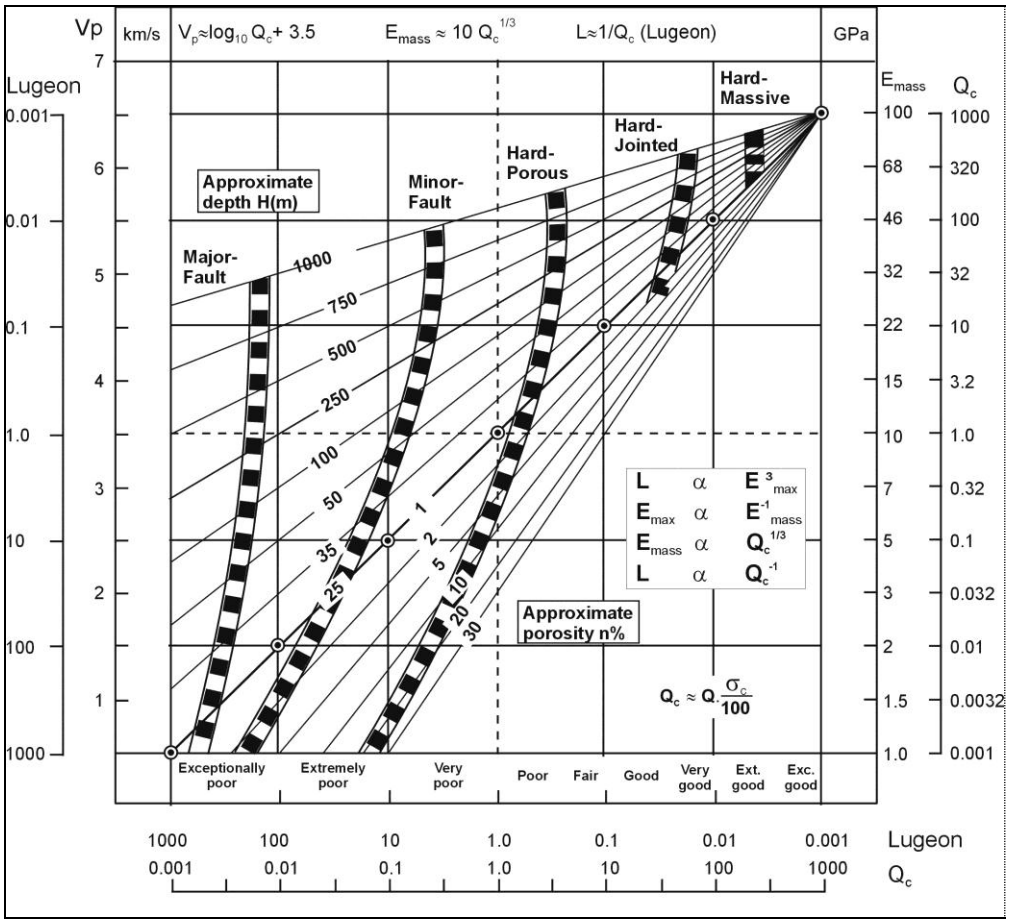

Fig. 16. An extension of Figure 12 to include very approximate estimates of Lugeon value, strictly for the case of rock masses without clay-filling (and therefore flow-blockage) of the joints. For a more general case, the modified term Q_{H2O} is used. This is shown in Figure 17. Note the 'type-curves' in the above figure for e.g. 'massive rock' and 'jointed rock'.

Table 1. A set of inter-related geotechnical approximations that are useful when assessing results in the field. Note: $Q_c = Q \times \sigma_c/100$. Barton, 2002, 2006.

Q_c	0.1	1	10	100
Lugeon	10	1	0.1	0.01
K (m/s) ≈	10^{-6}	10^{-7}	10^{-8}	10^{-9}
V_p (km/s)	2.5	3.5	4.5	5.5

It is noted in recent work from Sweden (Svensk Kärnbränslehantering AB, 2006) that the permeabilities at the Laxemar site in the range 10^{-4} to 10^{-9} m/s, based on 100 m test scales (in other words smoothed data, in relation to that obtained with close packer-spacing), shows the mean depth-variation given in Table 2.

Table 2. Smoothed permeability data from the Laxemar site in Sweden. (Svensk Kärnbränslehantering AB, 2006). Extreme values, even at 600-800 m depth, sometimes range from at least 10^{-6} to 10^{-11} m/s (where local variations in Q-value will also be likely.

K (m/s)	10^{-4}	10^{-5}	10^{-6}	10^{-7}	10^{-8}	10^{-9}
Depth (m)	≈ 20 m	≈ 30 m	≈ 50 m	≈ 100 m	≈ 300 m	≈ 900 m

Strictly considering the smoothed data, there is a certain indication of improved rock quality with depth, which of course is supported by extensive Q-logging of cores from deep boreholes in this jointed rock mass. Since stress levels are also increasing with rock quality, it is likely that other rock mechanics characterization data will also vary with depth, and indeed with direction.

Table 3 shows the previously described $L \approx 1/Q_c$ approximation for clay-free rock masses, and a more logical relation with permeability in general, that is obtained by a modified Q-calculation. The modification involves the inversion of Jr/Ja to the form Ja/Jr, whereby clay filling will result in an increase of Q_{H2O} (and a reduction of the permeability estimate), with increase in roughness or discontinuous jointing giving a similar effect. Figure 17 shows the depth-dependence that is presently built into the permeability estimate. As in the case of the Q_c-depth curves in Figure 15, one will usually experience curve-jumping as quality improves at depth. Q_{H2O} will tend to increase with depth, like Q_c, permeability thereby reducing.

Table 3 The two versions of 'Q-permeability' estimation. It should not need to be emphasised that both are approximate. Both are presently based on limited test data.

1) $L \approx 1/Q_c$ (1 Lugeon ≈ 10^{-7} m/s ≈ 10^{-14} m^2 for water at 20ºC) (*hard, jointed, clay-free,* rock masses)	**2)** *General case, with depth/stress allowance, and consideration of joint wall strength JCS*
Q_c = RQD/Jn x Jr/Ja x Jw/SRF x σ_c/100 (standard equation, normalized by σ_c/100)	**Q_{H2O} = RQD/Jn x *Ja/Jr* x Jw/SRF x 100/JCS** **K ≈ 0.002 /(Q_{H20} $D^{5/3}$) m/s**

Example of Q_{H2O} estimation: Weak, well-jointed rock at 100 m depth with a low assumed joint-wall-compression-strength JCS of 10 MPa:

Regular Q-value =

$$\frac{50}{9} \times \frac{1.5}{4} \times \frac{0.66}{1}$$

= 1.4, i.e. 'poor'

$$Q_{H_2o} = \frac{50}{9} \times \frac{4}{1.5} \times \frac{0.66}{1} \times \frac{100}{10} = 98$$

$$K \approx \left(\frac{2}{1000 \times 98 \times 100^{5/3}} \right) = 9 \times 10^{-9} \text{ m/s}$$

(Quite low permeability despite the extensively jointed nature of this rock mass, due to nearly closed, compressible, clay-coated joint walls).

This model can be extrapolated to many kilometres depth by those familiar with the operations of SRF in the Q-system. Naturally, where SRF attains high *classification* ratings in highly stressed (previously) massive rock, a low value of Q_{H2O} would be predicted, giving an assumed increased estimate of permeability in such an EDZ.

ROCK MASS VARIABILITY: SIMPLICITY VERSUS COMPLEXITY

Widely contrasting rock mass qualities that may challenge both the civil and mining professions are shown in Figure 18. The highly jointed, clay-bearing and weathered core is from a project that has not been *completed* during thirteen years of trying, due to some 500 m of similarly sheared and clay-bearing rock, also with too much water. The second project may not be *started* for at least ten years. The first should already have been passing high-speed trains, the other may have high-level nuclear waste some time in the future. They are both from the same country, but may have six orders of magnitude contrast in Q-value. This seems logical in relation to relative construction-difficulty, strength and deformation properties of the very different materials.

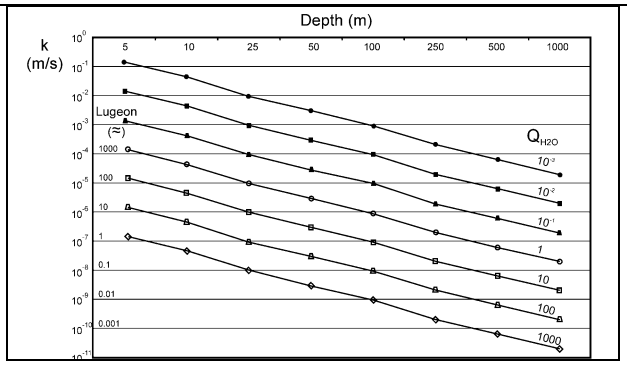

Fig. 17. Depth-dependent permeability estimation using Q_{H2O} concept. (Table 3, equation 2). As in the case of the Q_c-depth curves in Figure 15, one will usually experience curve-jumping as quality improves at depth. Q_{H2O} will tend to increase with depth, like Q_c.

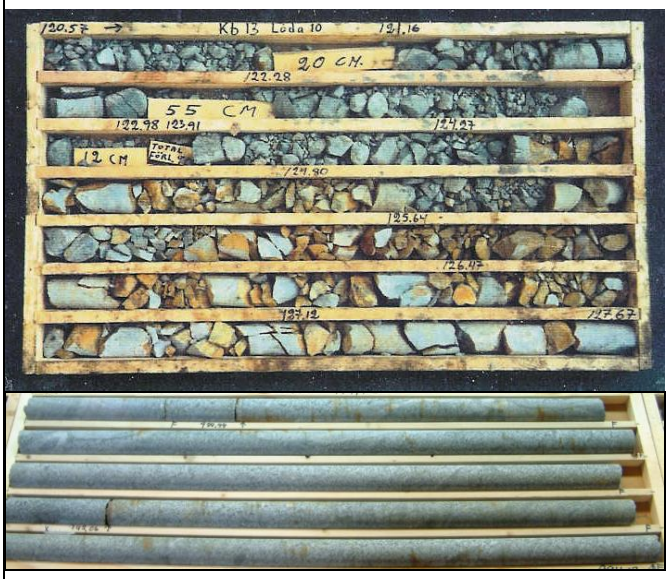

Fig. 18. The contrast shown by these two core boxes suggests orders of magnitude differences in quality. Individual quantitative descriptions of shear strength and deformation modulus would also vary by orders of magnitude. There is little logic in ratings of about 5 and 95 to describe these cases.

The six-orders-of-magnitude range of Q is a partial reflection of the potentially enormous variability of geology and structural geology. It is probably because of the relative sensitivity of a classification that can show wide numerical variation (i.e. 10-3 to 103, or an even wider range using Qc = Q x σc/100), that correlation with a very varied geologic and hydro-geologic reality is achieved, using rather simple correlations. Some of course would claim that the correlations are too simple. Without this range of Q (approx. 106) or Qc (approx. 109), correlation would anyway be more complex.

INPUT DATA FOR MODELS FROM ROCK MASS CLASSIFICATION

A long time ago, in the late 1960's, there was a move in some rock mechanics circles to try to move beyond the confines of continuum modelling, and focus on the possible effects of jointing on the performance and reinforcement needs of rock excavations, be they tunnels, slopes or dam abutments.

Thanks to the late 1960's modelling developments of Goodman and his colleagues with joint elements in FEM codes, followed by Cundall in the early 1970's, first with µDEC, then UDEC and later with 3DEC, this focus could be fulfilled by an increasing number of rock mechanics practitioners around the world. However, utilizing these codes correctly, with realistic input data, needs experience, time and therefore budgets to match. Ironically, input data for some continuum codes seems now to be considerably more complex than for discontinuum codes, as suggested in Figure 18.

GSI-based Hoek-Brown formulations for *'simple'* geotechnical input data for the rock mass, shown in Figure 19, such as deformation modulus, cohesion and friction angle, appear to have reached 'black-box' levels of complexity, which seems to be detrimental to the idea of rock engineering, if engineering judgement is still to be exercised in this rewarding field of engineering.

There is no possibility to have any feel for the influence of local rock quality on the rock mass compression strength, friction angle or cohesion, when formulations require software, rather than estimation for their evaluation. The formulae on the left cannot be considered 'empirical' anymore, with the exception of the first equation for estimating modulus.

Presumably as a result of time and budgetary pressures, and also the developing need to model large-scale mining problems, there has been a marked trend for using *'convenient'* continuum codes, which also have particularly good graphics representation of results. Simple software packages for handling the complex input data calculations (e.g. Figure 19) are also provided, so that a smart user might theoretically need only limited understanding of rock mechanics principles to use the codes 'successfully'.

The writer has often used the 'Chinese method' of rapidly left-thumbing from the back of a consultant's report to the front, whereby the coloured appendices of endless stress distributions and deformation patterns, can be read almost as in a film.

$E_m\ (\text{GPa}) = \left(1-\frac{D}{2}\right)\sqrt{\frac{\sigma_{ci}}{100}} \times 10^{(GSI-10)/40}$	$E_m \approx 10 \times Q_c^{1/3}$
$\sigma'_{cm} = \sigma_{ci} \times \frac{(m_b + 4s - a(m_b - 8s))(m_b/4 + s)^{a-1}}{2(1+a)(2+a)}$	$\sigma_{cm} \approx 5\gamma Q_c^{1/3}$
$\phi' = a\sin\left[\frac{6am_b\left(s + m_b\sigma'_{3n}\right)^{a-1}}{2(1+a)(2+a) + 6am_b\left(s + m_b\sigma'_{3n}\right)^{a-1}}\right]$	$"\phi" \approx \tan^{-1}\left(\frac{J_r}{J_a} \times \frac{J_w}{1}\right)$
$c' = \frac{\sigma_{ci}\left[(1+2a)s + (1-a)m_b\sigma'_{3n}\right]\left(s + m_b\sigma'_{3n}\right)^{a-1}}{(1+u)(2+a)\sqrt{1 + \left(6am_b\left(s + m_b\sigma'_{3n}\right)^{a-1}\right)\Big/\left((1+a)(2+a)\right)}}$	$"c" \approx \left(\frac{RQD}{J_n} \times \frac{1}{SRF} \times \frac{\sigma_c}{100}\right)$

Fig. 19. The extraordinarily complex formulae (left), for developing input data for some recent continuum models, and comparison to some of the less developed, and equivalent Q-based formulae.

Table 4. Five hypothetical rock masses with reducing quality from top to bottom of the tabulation. Note the difference between Q and Q_c due to normalization by $\sigma_c/100$. The sensitive, logical values of FC and CC already exist in the Q_c calculation, requiring no further empiricism.

RQD	J_n	J_r	J_a	J_w	SRF	Q	σ_c	Q_c	*FC°*	*CC* MPa	V_p km/s	E_{mass} GPa
100	2	2	1	1	1	100	100	100	63°	50	5.5	46
90	9	1	1	1	1	10	100	10	45°	10	4.5	22
60	12	1.5	2	0.66	1	2.5	50	1.2	26°	2.5	3.6	10.7
30	15	1	4	0.66	2.5	0.13	33	0.04	9°	0.26	2.1	3.5
10	20	1	6	0.5	5	0.008	10	0.0008	5°	0.01	0.4	0.9

Does all this 'colour' represent anything real? Would the numerical modellers know how to input a neglected clay seam – without 'smoothing-it-out' in a continuum approximation? Would the complex estimates of c' and φ' in Figure 19 change very much?

CC AND FC: THE COHESIVE AND FRICTIONAL COMPONENTS OF Q_C

In Figure 19, simple Q-based equations for 'c' and 'φ' were shown, that are actually found to be composed of each 'half' of the Q_c-formulation. They have the advantage of not requiring software for their calculation – they already exist in the calculation of the Q_c value. They are defined as follows:

'cohesive component' CC = RQD/Jn × 1/SRF × $\sigma_c/100$

'frictional component' FC = $\tan^{-1}$[Jr/Ja × Jw]

Examples of these rock mass component strengths are given in Table 4, for a range of possible Q-values for increasingly jointed rock masses. The P-wave velocity and (pseudo-static) deformation modulus estimates are from the central diagonal, near-surface (25 m depth) inter-relationships given in Figure 12. They could equally well be quoted for greater depths, if more relevant.

Plate loading tests taken to such high stress levels that *rock mass failure* occurs are rare. However, measurement of P-wave velocity at such sites may allow tentative extrapolation to other sites through a common rock mass quality estimate. Such data can then be a source of tentative rock mass strength ($\sigma_{c\ mass}$) estimation.

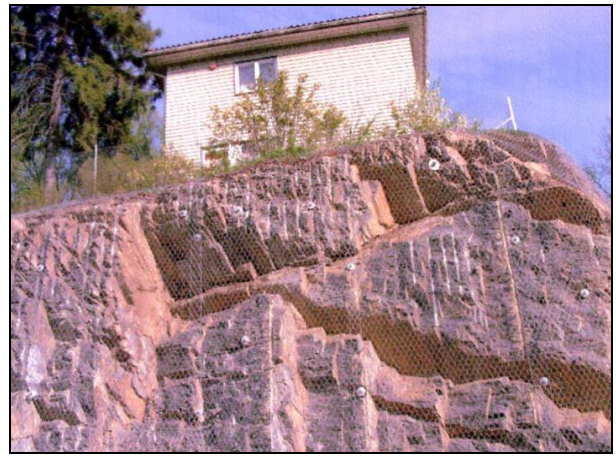

Fig. 20. Examples of rock masses with particularly low CC (left), and particularly low FC (right). These require relatively more shotcrete (left) and relatively more bolting (right). The original Q-system case records have apparently reflected these different needs, and the Q-parameter ratings developed have given the possibility of realistic CC and FC values.

Table 5 suggests compressive (and cohesive) strengths in rock masses somewhat higher than those usually assumed. They also show some implicit variation from the values set up in Table 4 (from specific Q-parameter combinations), but reinforce the idea of potentially very high cohesive strengths (e.g.10's of MPa) in competent rock masses. This table of values seems to imply very different values of cohesion to some of the earlier RMR-based estimates of cohesion for rock masses, where 'c' was generally given as < 1 MPa for a wide range of RMR.

Table 5. Plate load tests driven to failure, with corresponding velocity and modulus data for the different rock masses. (Savich et al., 1974)

Velocity V_p (km/s)	2.3	3.7	4.0
Modulus E_{mass} (GPa)	1	3	15
Rock mass σ_{cm} (MPa)	4	20	50

One should note, when discussing 'c' and 'φ', that shear strength criteria of the form 'c + tan φ' used in continuum codes, for predicting so-called 'plastic zones' due to stress-induced failure of rock around a tunnel, will in reality suffer cohesion reduction at small strain, and friction mobilization at larger strain. Mohr-Coulomb and Hoek-Brown strength criteria need to be modified to the form 'c *then* tan φ' for more correct determination of the so-called 'plastic zones'. At present, stress-induced break-out is not correctly modelled by such codes. 'Plastic zones' are exaggerated, and bolt lengths related to such calculations may have little practical use, as 'failure' is not correctly linked to stress redistribution effects.

CONCLUSIONS

Shallow seismic refraction and cross-hole seismic measurements are powerful means of extrapolating rock quality , and investigating local variations in detail. In this paper, velocity measurements have been demonstrated that help to quantify the EDZ phenomenon that is a part of the classification of the effect of excavation, and also the velocities without excavation, which would correspond with the broader goal of characterization, prior to project start-up. The differences need to be described in rock mass quality descriptors such as RMR and Q.

An integration of the Q-value with seismic and permeability data has been described because there is a limit to how many boreholes can be drilled, how many cores can be logged, and how many permeability tests can be performed. The ability to extrapolate these 'point sources' of information helps to project rock quality classes along a tunnel, or to different parts of a large cavern or mine.

Due to the effect of increased stress at greater tunnel or cavern depth, it must be expected that deformation modulus and seismic velocity will also increase. Eventual sonic logging or cross-hole tomography ahead of a tunnel face may therefore give a higher velocity than the rock quality may suggest.

The simplest approximation for permeability is that the number of Lugeon: $L \approx 1/Q_c$. This is strictly for the case of clay-free, jointed, low porosity rock masses. A more generally applicable approximation using the term Q_{H2O}, uses an

inverted Ja/Jr term and 100/JCS to give a better link to permeability. A high value of Q_{H2O}, and of Q_c, implies low permeability. An empirically determined general reduction of permeability with depth is also modelled. This new method shows promise, but needs more data.

Strength criteria of the form 'c + tan φ' used in continuum codes, with links to GSI, have recently acquired remarkable complexity and require software for evaluation of their components. Sight may be lost of the influence of the frequent anisotropic details of the rock mass, such as clay-filled discontinuities.

The terms CC and FC from the Q-calculation show promise in giving a direct preliminary estimate of the magnitudes of rock mass cohesive and frictional strength, with 'immediate' reaction to anisotropic details, and a certain sensitivity to orientation in RQD and Jr/Ja.

Logic would suggest that the CC and FC components should also not be *added* in an eventual failure criterion, as 'c + tan φ' does not correctly match stress-induced failure, due to degradation of 'c' and mobilization of 'tan φ' at widely different strains.

The wide range of Q-values (0.001 to 1000) and the even wider range of Q_c (0.00001 to 5000) reflects *to some degree* the very wide range of geological conditions, and is probably responsible for the fact that empirical equations, such as links to velocity and deformation modulus, are particularly simple. This does not mean that they cannot be improved, but simplicity should be maintained if possible.

REFERENCES

Aydan, Ö., Akagi, T., Ito, T. & Kawamoto, T. 1992. Prediction of behaviour of tunnels in squeezing ground. *Journal of Geotechnical Engineering*. *448*:*III-19:* 73-82. JSCE.

Barton, N., By, T.L., Chryssanthakis, P., Tunbridge, L., Kristiansen, J., Løset, F., Bhasin, R.K., Westerdahl, H. & Vik, G. 1994. Predicted and measured performance of the 62m span Norwegian Olympic ice hockey cavern at Gjøvik. *Int. J. Rock Mech, Min. Sci. & Geomech. Abstr*., *31:6:* 617-641. Oxford: Pergamon.

Barton, N. 2002. Some new Q-value correlations to assist in site characterization and tunnel design. *Int. J. Rock Mech. & Min. Sci.* Vol. 39/2:185-216.

Barton, N. 2006. *Rock Quality, Seismic Velocity, Attenuation and Anisotropy*. Taylor & Francis, London & Netherlands, 629 p.

Barton, N. 2007a. Thermal over-closure of joints and rock masses and implications for HLW repositories. Proc. of *11th ISRM Congress,* Lisbon.

Barton, N. 2007b. Near-surface gradients of rock quality, deformation modulus, Vp and Qp to 1km depth. First Break, *EAGE*,October, 2007, Vol. 25, 53-60.

Bonapace, B. 1983. Tests and measurements for the pressure tunnels and shafts of the Sellrain-Silz hydroelectric power scheme with extremely high head. *International Society for Rock Mechanics. International Congress, 5. Melbourne 1983. 2:* D287-D292. Rotterdam: Balkema.

Bieniawski, Z.T. 1989. Engineering rock mass classifications: A complete manual for engineers and geologists in mining, civil and petroleum engineering. 251 p. J. Wiley.

Fourmaintraux, D. 1995. Quantification des discontinuités des roches et des massifs rocheux. *Rock Mechanics, 7:* 83-100. Springer-Verlag.

Hudson, J.A., Jones, E.J.W. & New, B.M. 1980. P-wave velocity measurements in a machine-bored, chalk tunnel. *Q. Jl Engng Geol.,13:* 33-43. Northern Ireland: The Geological Society.

Ishikawa, K., Ochi, H. & Tadaka, S. 1995. Rock mass classification of weathered granite and evaluation of geomechanical parameters for bridge foundation of large scale structure in the Honshu-Shikoku Bridge Authority. Rock Foundation. *International Workshop on Rock Foundation.* Tokyo 1995. 169-176. Rotterdam: Balkema.